Expression of Ror2 Associated with Fibrosis of the Submandibular Gland

Takahashi, Daiki ; Suzuki, Hiroaki ; Kakei, Yasumasa ; Yamakoshi, Kimi ; Minami, Yasuhiro ; Komori, Takahide ; Nishita, Michiru

(Citation)
Cell Structure and Function,42(2):159-167

(Issue Date)
2017

(Resource Type)
journal article

(Version)
Version of Record

(URL)
https://hdl.handle.net/20.500.14094/90005598

CELL STRUCTURE AND FUNCTION 42: 159–167 (2017)

Expression of Ror2 Associated with Fibrosis of the Submandibular Gland

Daiki Takahashi[1,2], Hiroaki Suzuki[2], Yasumasa Kakei[2], Kimi Yamakoshi[3], Yasuhiro Minami[1], Takahide Komori[2], and Michiru Nishita[1]***

[1]*Division of Cell Physiology, Department of Physiology and Cell Biology, Kobe University, Graduate School of Medicine, 7-5-1, Kusunoki-cho, Chuo-ku, Kobe, Hyogo 650-0017, Japan,* [2]*Department of Oral and Maxillofacial Surgery, Kobe University, Graduate School of Medicine, 7-5-1, Kusunoki-cho, Chuo-ku, Kobe, Hyogo 650-0017, Japan,* [3]*Department of Mechanism of Aging, Research Institute, National Center for Geriatrics and Gerontology, 7-430, Morioka, Obu, Aichi 474-8511, Japan*

ABSTRACT. **The submandibular gland (SMG) is one of the major salivary glands that play important roles for variety of physiological functions, such as digestion of foods, prevention of infection, and lubrication of the mouth. Dysfunction of the SMG, often associated with a salivary inflammation, adversely influences a person's quality of life. However, the mechanism underlying inflammation-driven dysfunction of the SMG is largely unknown. Here, we used a mouse model in which the main excretory duct of the SMG is ligated unilaterally to induce inflammation of the gland and examined the expression of *Wnt5a*, *Ror1* and *Ror2* genes, encoding Wnt5a ligand and its cognate receptors, which have been implicated in tissue damage or inflammatory responses in variety of tissues. We show that expression levels of *Ror1*, *Ror2*, and *Wnt5a* are increased in the ligated SMG undergoing interstitial fibrosis, which is accompanied by robust expression of fibrosis-associated genes, such as *TGF-β1*, *TNF-α*, *IL-1β*, and *MMP-2*. Increased immunostaining signal of Ror2 was detected in the fibrotic tissues with abundant accumulation of fibroblasts and collagen fibers in the ligated SMG, suggesting that Ror2-mediated signaling might be activated in response to tissue damage and associated with progression of fibrosis in the SMG.**

Key words: submandibular gland, Ror2, Wnt5a, fibrosis, inflammation

Introduction

The Wnt family of secreted glycoproteins play crucial roles in various cellular functions by activating either β-catenin-dependent (canonical) or -independent (non-canonical) signaling pathway (He *et al.*, 2004; Hurlstone and Clevers, 2002; Kikuchi and Yamamoto, 2008; Kohn and Moon, 2005; Veeman *et al.*, 2003; Wodarz and Nusse, 1998). Wnt5a is a representative Wnt protein that can activate non-canonical Wnt signaling through its binding to the Ror family of receptor tyrosine kinases, which consist of two structurally related members, Ror1 and Ror2 (Endo *et al.*, 2015; Minami *et al.*, 2010; Nishita *et al.*, 2010).

Wnt5a, Ror2 as well as Ror1 have been implicated in tissue-damage and inflammatory responses in adult tissues. For example, expression of Wnt5a and Ror2 is induced in the damaged kidney after unilateral ureteral obstruction (UUO), leading to renal fibrosis in mice (Li *et al.*, 2013). Ror2-mediated signaling seems to elicit expression of MMP-2, thereby disrupting the tubular basement membrane in the kidney (Li *et al.*, 2013). Expression of Ror2 is also induced in reactive astrocytes following brain injury to promote their proliferation in mice, which is important for the formation of glial scars during the tissue repair (Endo *et al.*, 2017). Furthermore, in demyelinating disorders, inflammatory cytokines released from activated microglia induce expression of Ror2 in neurons, contributing to the progression of neurodegeneration (Shimizu *et al.*, 2016). Wnt5a-Ror2 signaling has also been shown to promote dextran sodium sulfate (DSS)-induced colitis by enhancing pro-inflammatory cytokine production in the colon (Sato *et al.*, 2015). More recently, we have shown that Ror1 is expressed inducibly in satellite cells by inflammatory cyto-

*To whom correspondence should be addressed: Michiru Nishita, Department of Physiology and Cell Biology, Graduate School of Medicine, Kobe University, 7-5-1, Kusunoki-cho, Chuo-ku, Kobe 650-0017, Japan.
Tel: +81–78–382–5561, Fax: +81–78–382–5579
E-mail: nishita@med.kobe-u.ac.jp
**To whom correspondence should be addressed: Yasuhiro Minami, Department of Physiology and Cell Biology, Graduate School of Medicine, Kobe University, 7-5-1, Kusunoki-cho, Chuo-ku, Kobe 650-0017, Japan.
Tel: +81–78–382–5561, Fax: +81–78–382–5579
E-mail: minami@kobe-u.ac.jp

Abbreviations: Ctgf, connective tissue growth factor; ECM, extracellular matrix; HE, hematoxylin and eosin; IL-1β, Interleukin 1β; MMP, matrix metalloproteinase; qRT-PCR, quantitative real-time PCR; SMG, submandibular gland; TGF-β, Transforming growth factor-β; TNF-α, Tumor necrosis factor-α; UUO, unilateral ureteral obstruction.

kines in the injured skeletal muscles and promotes its proliferation, required for skeletal muscle regeneration (Kamizaki *et al.*, 2017).

The submandibular gland (SMG) is one of the major salivary glands (Pedersen *et al.*, 2002). Saliva has a variety of physiological functions, such as digestion of foods, prevention of infection, and lubrication of the mouth. Salivary inflammation, often associated with Sjögren's syndrome and radiotherapy of head and neck cancers, causes dysfunction of the salivary glands, adversely influencing a person's quality of life (Fox *et al.*, 2000; Henson *et al.*, 2001; Murakami *et al.*, 2015). Current treatments for the salivary dysfunction are limited to the administration of saliva substitutes and sialogogues (Vissink *et al.*, 2010).

Here we used a mouse model in which the main excretory duct of the SMG is ligated unilaterally to induce salivary inflammation. We show that expression levels of *Ror1*, *Ror2*, and *Wnt5a* are increased in the ligated SMG undergoing interstitial fibrosis, which is accompanied by robust expression of fibrosis-associated genes, such as *TGF-β1*, *TNF-α*, *IL-1β*, and *MMP-2*. Increased immunostaining of Ror2 was detected in the fibrotic tissues with abundant accumulation of fibroblasts and collagen fibers in the ligated SMG, suggesting that Ror2-mediated signaling might be activated in response to tissue damage and associated with progression of fibrosis in the SMG.

Materials and Methods

Animals

All the experiments using animals in this study were approved by the Institutional Animal Care and Use Committee (Permission number: P160401) and carried out according to the Kobe University Animal Experimentation Regulations. Male *C57BL/6J* mice (8 weeks of age) obtained from Japan SLC (Shizuoka, Japan) were used in the present study. Mice were anesthetized using isoflurane controlled by small-animal anesthetizer (TK-7, Biomachinery, Chiba, Japan). The main excretory duct of the right SMG was exposed through an incision in the neck and ligated with surgical suture (7-0 braided silk suture, Akiyama MFG, Tokyo, Japan). The main excretory ducts of the sham-operated mice were exposed and were not ligated. The mice were anesthetized and euthanized on day 1, 3, or 7 after the ductal ligation. The ligated, contralateral, and sham-operated glands were excised and processed for quantitative real-time PCR (qRT-PCR) and histological analyses as describe below.

qRT-PCR

Total RNAs were isolated from the SMGs by using Isogen (Nippon gene, Toyama, Japan) and reverse-transcribed using Prime Script 1'st strand cDNA synthesis kit (Takara, Kusatsu, Japan). qRT-PCR was performed on the LightCycler 480 system (Roche Diagnostics, Tokyo, Japan) using LightCycler 480 SYBR Green I Master (Roche Diagnostics). Relative mRNA levels of the respective genes of interest were determined after normalization with the levels of *18S* mRNA. Forward and reverse primer sets for PCR were as follows:

TNF-α, 5'-GGGGCCACCACGCTCTTCTGTC-3'
and 5'-TGGGCTACAGGCTTGTCACTCG -3';
*TGF-β*1, 5'- GGAGAGCCCTGGATACCAAC-3'
and 5'-CAACCCAGGTCCTTCCTAAA-3';
IL1-β, 5'- CAGGATGAGGACATGAGCACC-3'
and 5'-CTCTGCAGACTCAAACTCCAC-3';
MMP-2, 5'-CACCACCACAACTGAACCAC-3'
and 5'-CTCAGAAGAGCCCGCAGTAG-3' ;
Wnt5a, 5'-CAAATAGGCAGCCGAGAGAC-3'
and 5'-CTCTAGCGTCCACGAACTCC-3';
Ror1, 5'-GCTGCGGATTAGAAACCTTG -3'
and 5'- TACGGCTGACAGAATCCATC-3';
Ror2, 5'-TGGAACTGTGTGACGTACCC-3'
and 5'-GCGAGGCCATCAGCTG-3';
18S, 5'-CGATAACGAACGAGACTCTG -3'
and 5'-GACATCTAAGGGCATCACAG-3'.

The RT^2 Profiler PCR Array Mouse Fibrosis (PAMM-120 G-4; QIAGEN, Hilden, Germany) was used to examine the expression profiles of genes involved in fibrosis. Gene expression levels were analyzed by using the web-based software 'RT^2 Profiler PCR Array Data Analysis version 3.5', and relative mRNA levels of the respective genes of interest were determined after normalization with the levels of *GAPDH* mRNA.

Histological staining

The SMGs from the respective mice were fixed with 4% (w/v) paraformaldehyde at 4°C overnight and equilibrated with 30% (w/v) sucrose. The specimens were frozen in OCT compound (Sakura Finetek Japan, Tokyo, Japan) and cut into 10-μm sections. For hematoxylin and eosin (HE) staining, the sections were stained with Mayer's Hematoxylin (Muto pure chemicals, Tokyo, Japan) and 1% Eosin Alcohol Solution (Muto pure chemicals) for 5 min each. For Azan staining, the sections were incubated with 5% (v/v) trichloroacetic acid and 5% (v/v) potassium dichromate for 10 min, Azocarmine G Solution (Wako Pure Chemical Industries, Osaka, Japan) for 30 min, 0.1% (v/v) aniline in 70% (v/v) ethanol for 3 sec, 0.1% (v/v) acetic acid in 95% (v/v) ethanol for 1 min, 5% (w/v) phosphotungstic acid for 60 min, and Aniline blue-orange G solution (Wako Pure Chemical Industries) for 3 min. The slides were evaluated under the light microscope (BZ-X710; Keyence Corporation, Osaka, Japan).

Immunochemistry

The sections were permeabilized with 0.1% (v/v) Triton X-100 for 20 min, washed in PBS, and then immersed in 0.1% (v/v) hydrogen peroxide for 60 min. After washing with PBS and blocking with Blocking serum (VECTASTAIN ABC KIT; Vector Laboratories, Burlingame, CA, USA) for 60 min, the specimens were incu-

bated with anti-Ror2 rabbit polyclonal antibody (Kani *et al.*, 2004) diluted 1:100 in Can Get Signal immunostain Solution A (Toyobo, Osaka, Japan) overnight at 4°C, followed by incubation with biotinylated anti-rabbit IgG (Vector Laboratories) for 120 min at room temperature. The sections were incubated with VECTASTAIN ABC reagent (Vector Laboratories) for 60 min at room temperature, developed with DAKO ENVISION kit/HRP (DAB) (DAKO, Carpinteria, CA, USA), and counterstained with hematoxylin. The slides were evaluated under the light microscope (BZ-X710).

Immunofluorescence staining

The sections were permeabilized with 0.1% (v/v) Triton X-100 for 20 min and blocked with 5% (w/v) BSA for 60 min. The specimens were incubated with anti-vimentin antibody (D21H3; Cell Signaling Technology, Danvers, MA, USA) diluted 1:100 in Can Get Signal immunostain Solution B (Toyobo) overnight at 4°C and then with Alexa Fluor 546-conjugated anti-rabbit IgG (Invitrogen, Carlsbad, CA, USA) diluted 1:500 in Can Get Signal immunostain Solution B. The specimens were counterstained with DAPI and mounted with the Fluoro-KEEPER Antifade Reagent, Non-Hardening Type (Nacalai tesque, Kyoto, Japan). Fluorescent images were obtained using BZ-X710 and processed using Image J (National Institutes of Health, Bethesda, MD, USA).

Statistical methods

Data collection and statistical analyses were carried out with Excel 2013 (Microsoft Corporation, Redmond, WA, USA). The associations of each variable were tested by Student's *t*-test. A value of $p<0.05$ was considered statistically significant.

Results

Ductal ligation induces fibrosis within the SMG

We used a mouse model in which the main excretory duct of the SMG was ligated unilaterally to induce inflammation in the gland. The contralateral SMG and sham-operated SMG were used as controls. The SMGs of mice are composed primarily of acinar cells, intercalated ducts, granular convoluted tubules, striated ducts, and excretory ducts. One day after ligation, most of the ducts in the ligated SMGs were dilated, while acinar cells appeared to be unaffected by the ductal ligation (Fig. 1A). On day 4 and 7 after ligation, in the ligated SMGs epithelial cells of the dilated

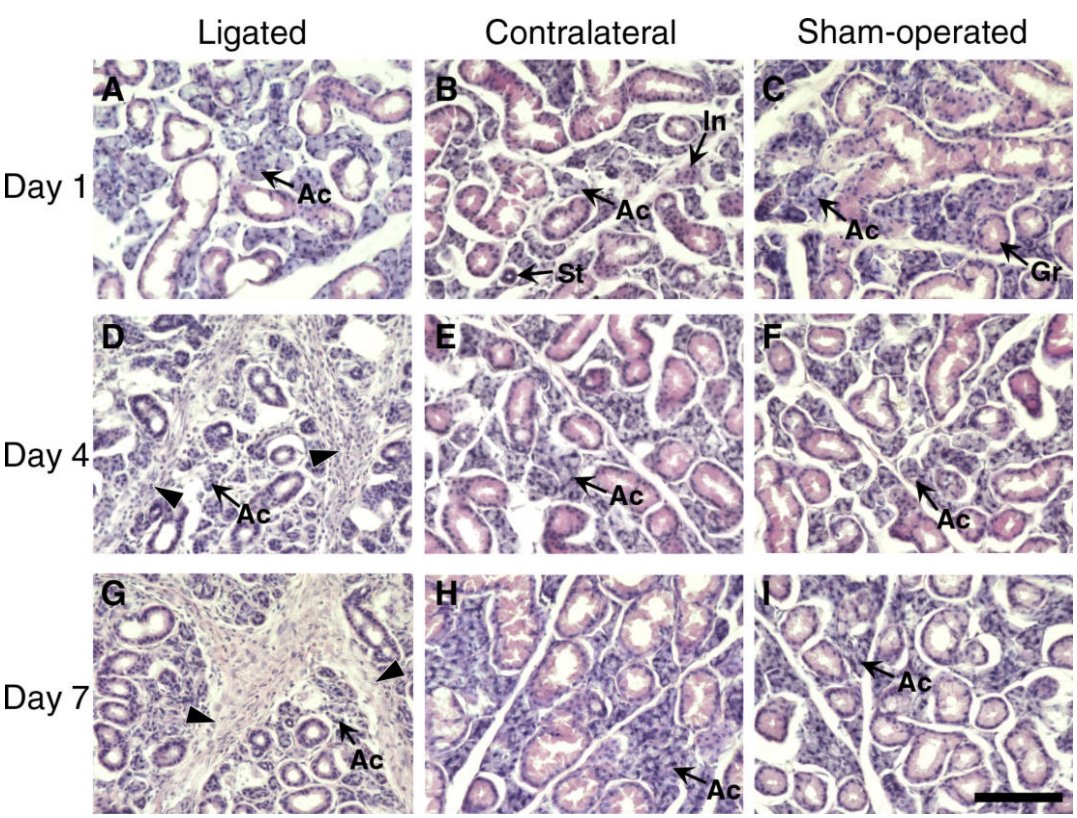

Fig. 1. HE staining of the ligated (A, D, G), contralateral (B, E, H), and sham-operated SMGs (C, F, I) on day 1 (A–C), day 4 (D–F), and day 7 (G–I) after the ductal ligation. The arrowheads indicate interlobular fibrotic lesions. Scale bar, 100 μm. Ac, acinar cells; St, striated duct; In, intercalated duct; Gr, granular convoluted tubule.

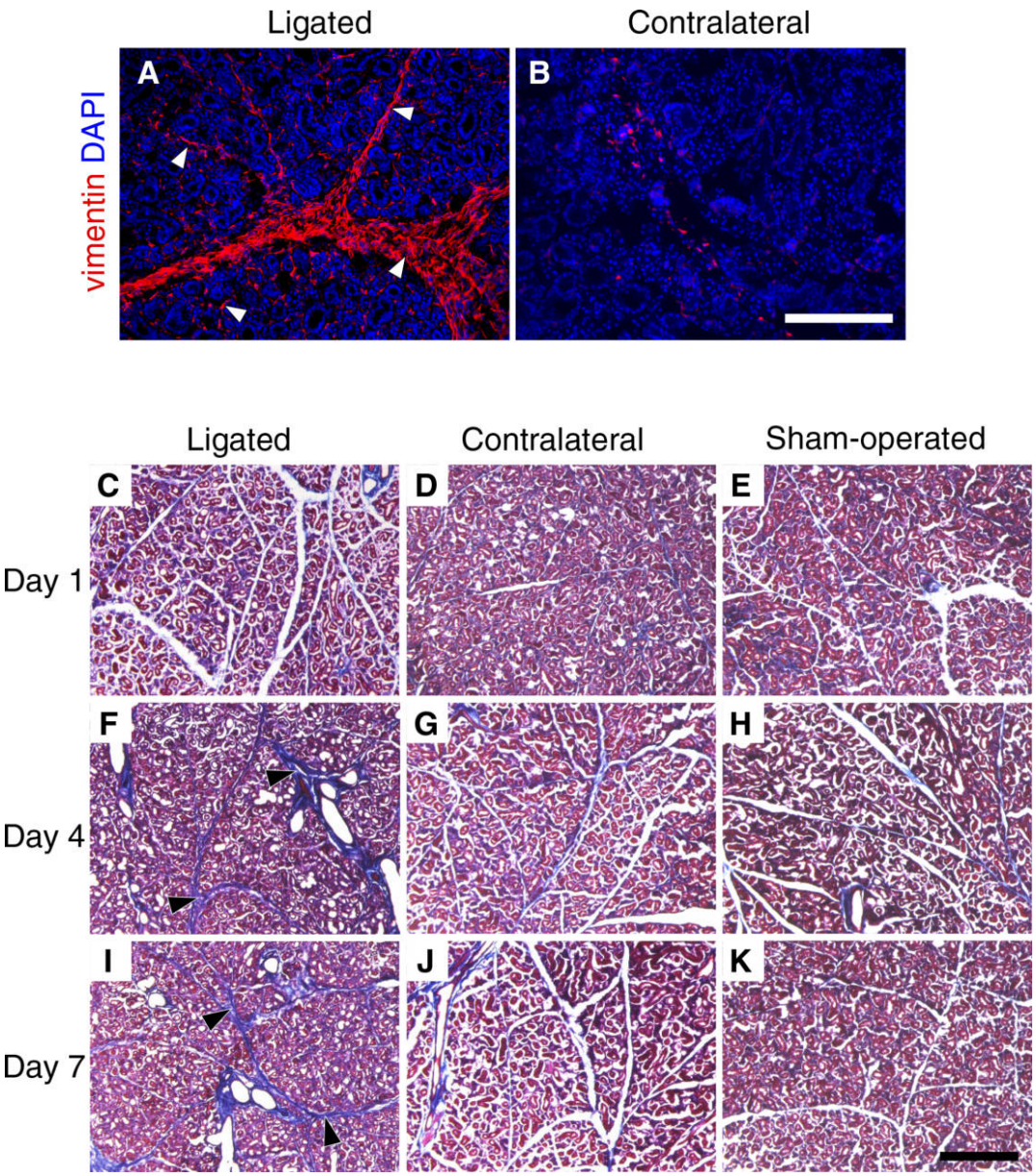

Fig. 2. Fibrosis within the SMGs induced by the ductal ligation. (A, B) Immunofluorescence staining of the ligated SMG (day 7) with anti-vimentin (red), showing accumulated vimentin-positive fibroblasts between and within the lobules in the ligated SMG (arrowheads), but not in the contralateral SMG. Scale bar, 200 μm. (C–K) Azan staining of the ligated (C, F, I), contralateral (D, G, J), and sham-operated SMGs (E, H, K) on day 1 (C–E), day 4 (F–H), and day 7 (I–K) after the ductal ligation. The arrowheads indicate interlobular collagen fibers stained in dark blue (F, I). Scale bar, 300 μm.

ducts as well as acinar cells were atrophied, and interstitial spaces between and within the lobules contained large number of fibroblast-like cells (Fig. 1D, G), which were not observed on day 1 (Fig. 1A). On the other hand, the contralateral and sham-operated SMGs failed to show any apparent alterations at any time points examined (Fig. 1B, C, E, F, H, I).

We next examined whether inflammation within the SMGs, induced by the ductal ligation, would bring about fibrotic lesions. Immunofluorescence staining with anti-vimentin antibodies revealed that the fibroblast-like cells, characterized by vimentin expression, were accumulated markedly between and within the lobules on day 7 of the ligated SMG, while such vimentin-positive cells were detected marginally in the contralateral SMG (Fig. 2A, B), indicating that the ductal ligation induces a robust increase in fibroblasts or fibroblast-like cells in interstitial tissues of the SMGs. Since increased fibroblasts are associated with

fibrotic lesions within damaged tissues, we examined the ligated SMGs by azan staining that identifies collagen fibers. In agreement with the distribution of fibroblasts, marked depositions of collagen fibers were detected between and within the lobules of the SMG on day 4 and 7, but not day 1, after the ductal ligation (Fig. 2C-K), indicating that the ductal ligation might induce fibrotic lesions or fibrosis within the SMGs.

Ductal ligation induces expression of Ror2 in fibrotic tissues

To study a possible involvement of Wnt5a-Ror signaling in damage responses within the SMG, expression levels of *Ror1*, *Ror2* and *Wnt5a* within the SMGs after the ductal ligation were examined by qRT-PCR. We found that expression levels of all of these genes are increased significantly on day 4 and 7, but not day 1, after the ductal ligation, compared to the respective contralateral SMGs (Fig. 3). There were not any apparent differences in these expression levels in the contralateral and sham-operated SMGs throughout the time course examined (Fig. 3). We next examined expression pattern of Ror2 in the ligated SMG by immunohistochemical analysis. Immunostining signals of Ror2 were detected in most of the ductal cells, but not acinar cells, of both ligated and control (contralateral and sham-operated) SMGs, irrespective of the periods of ligation (Fig. 4). Obviously, on day 4 and 7, but not day 1, Ror2 expression was increased markedly at the interstitial spaces between and within the lobules, and the Ror2-positive fibroblast-like cells were juxtaposed to the atrophied acinar cells (Fig. 4). Such increase in Ror2-expressing cells was not observed in the respective contralateral or sham-operated SMGs (Fig. 4). Thus, increased Ror2 expression seems to be correlated with the progression of fibrosis within the ligated SMG.

Effect of the ductal ligation on expression of fibrosis-related genes in the SMG

To explore the molecular nature of the SMG fibrosis, gene expression profiling of the ligated SMGs (day 7) was performed using a fibrosis PCR array. Genes whose expression was increased or decreased at least 2-fold in the ligated SMGs, compared to the respective contralateral SMGs, are shown in Table I. As expected from their key roles in regulating fibrosis of various organs (Liu, 2006; Mallat and Lotersztajn, 2013; Tatler and Jenkins, 2012; Thenappan *et al.*, 2010), expression of *Transforming growth factor-β (TGF-β) ligands*, *TGF-β1* and *TGF-β3*, were upregulated in the ligated SMGs (Table I). We also detected increased expression of the components and target genes of TGF-β signaling, such as *TGF-β receptor II*, *TGFB-induced factor homeobox 1*, *Smad7*, *Serpine1*, *connective tissue growth factor* (*Ctgf*), and *Snail1* (Table I), suggesting that TGF-β

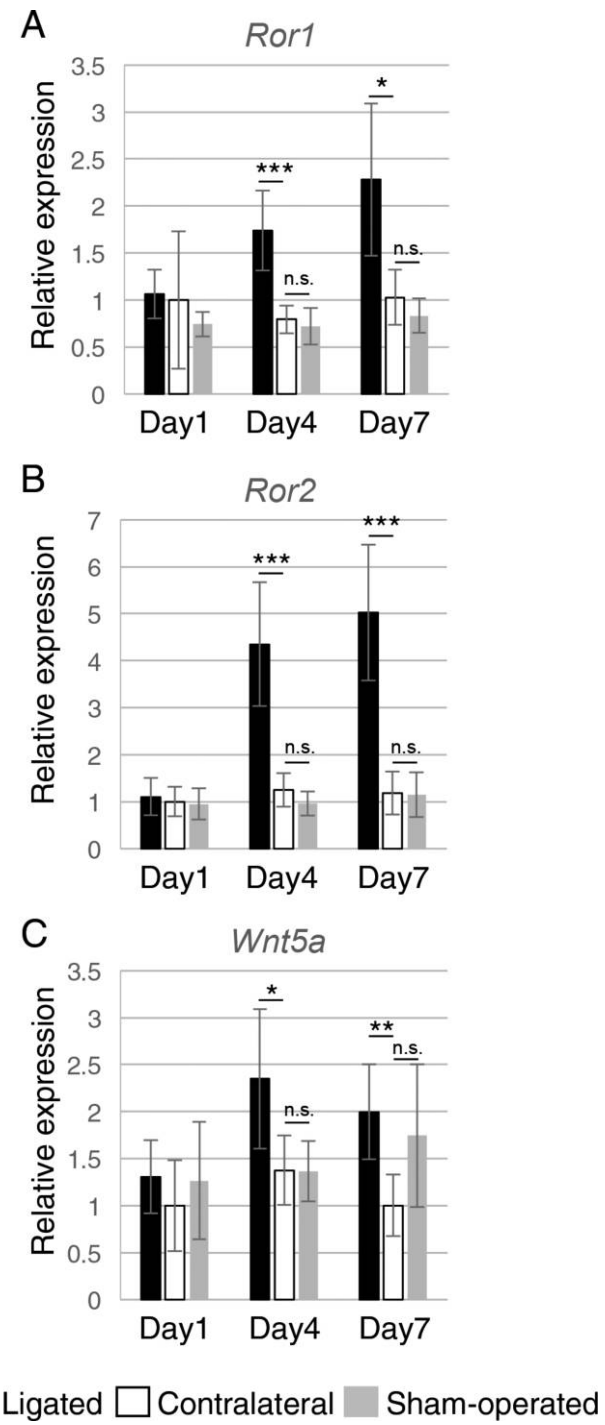

Fig. 3. Effects of the ductal ligation on expression levels of *Ror1*, *Ror2* and *Wnt5a*. The ligated and contralateral SMGs were isolated on day 1, 4, and 7 after the ductal ligation and analyzed by qRT-PCR. Data represent means±SD (n=6). *P<0.05; **P<0.005; ***P<0.0005, n.s.=not significant, *t* test.

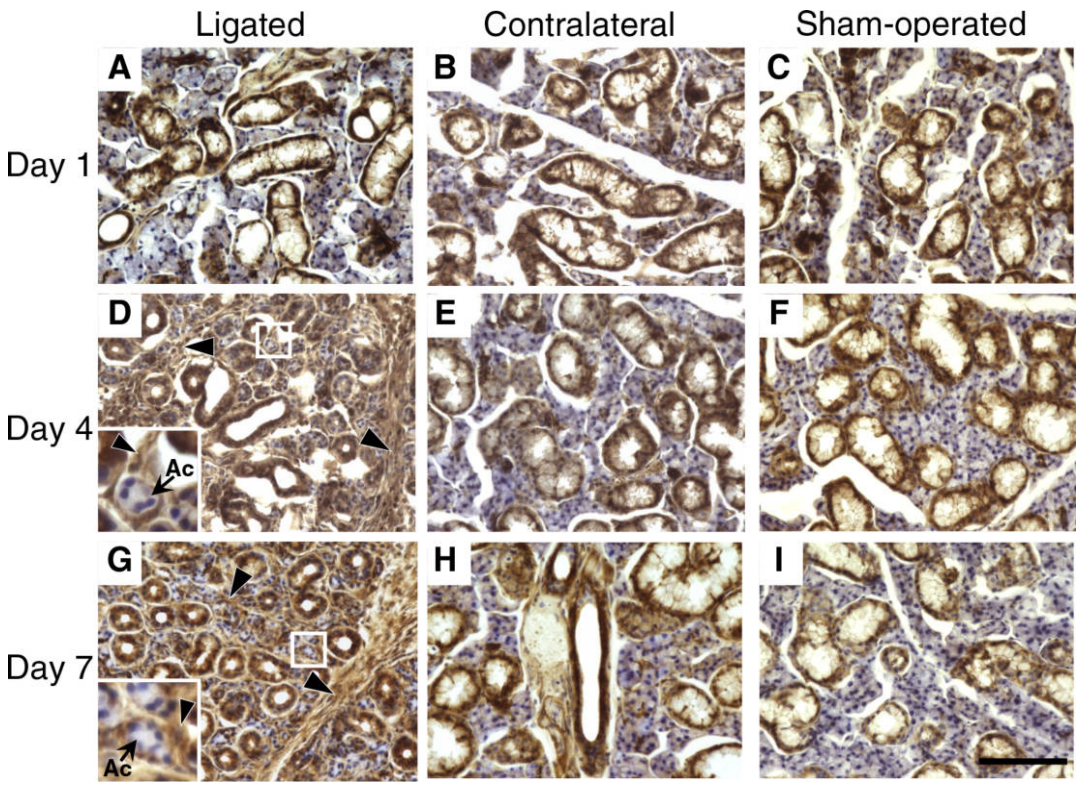

Fig. 4. Immunohistochemical analysis of Ror2 in the ligated (A, D, G), contralateral (B, E, H), and sham-operated SMGs (C, F, I) on day 1 (A–C), day 4 (D–F), and day 7 (G–I) after the ductal ligation. Immunostaining signals of Ror2 are markedly increased at the interstitial spaces between and within the lobules on day 4 and day 7 in the ligated SMGs (arrowheads), but not in the contralateral and sham-operated SMGs. Insets show magnified images of boxed regions. Scale bar, 100 μm. Ac, acinar cells.

signaling plays roles in regulating fibrosis of the ligated SMGs. The data of expression profiling further identified increased expression of genes involved in inflammatory response (e.g. *Interleukin 1β* (*IL-1β*) and *Tumor necrosis factor-α* (*TNF-α*)), extracellular matrix (ECM) remodeling (e.g. *Collagen type I* and *matrix metalloproteinases* (*MMPs*)), cell adhesion (e.g., *Integrin β8* and *Integrin αV*), and cell growth (e.g., *Platelet derived growth factor B* and *Hepatocyte growth factor*) (Table I).

We also examined the expression of *TGF-β1*, *TNF-α*, *IL-1β*, and *MMP-2* on day 1, day 4, and day 7 after the ductal ligation by qRT-PCR. Expression of *TGF-β1* and *TNF-α* was upregulated significantly in the ligated SMGs on day 1, and their levels were further increased on day 4 and day 7, compared to the respective contralateral SMGs (Fig. 5A, B). Significant increases in expression levels of *IL-1β* and *MMP-2* were observed in the ligated SMGs on day 4 and day 7 (Fig. 5C, D).

Discussion

Here, we found that expression of *Ror1*, *Ror2*, and *Wnt5a* was upregulated at mRNA levels during fibrosis of the SMG induced by the ligation of the main excretory ducts. Immunohistochemical analyses also revealed that expression of Ror2 was upregulated primarily at the interstitial spaces between and within the lobules, where fibroblastic cells, fibroblasts and collagen fibers were accumulated, following the ductal ligation, indicating that these fibroblasts express Ror2. Tissue fibrosis is a common cause of dysfunctions and diseases in various organs, including the SMG (Shimizu *et al.*, 2013). *TGF-β* has been shown to play key roles in the regulation of fibrosis in various organs (Liu, 2006; Mallat and Lotersztajn, 2013; Tatler and Jenkins, 2012; Thenappan *et al.*, 2010), and in fact, our PCR array data indicated an upregulation of *TGF-β1* and *TGF-β3* as well as their target genes in the ligated SMGs, consistent with the previous report (Woods *et al.*, 2015). We also found that increased expression of *TGF-β1* could be detected as early as day 1 after the ductal ligation, the time point when apparent increases in the expression of *Ror1*, *Ror2*, and *Wnt5a* were not detectable, suggesting that *TGF-β1* is involved primarily in early steps during tissue damage responses. In agreement with this notion, expression of *TGF-β1* is induced at earlier steps than expression

Table I. Genes differentially expressed in the ligated SMGs

Symbol	Description	Fold change
Serpine1	Serine (or cysteine) peptidase inhibitor, clade E, member 1	41.06
Lox	Lysyl oxidase	31.85
Col1a2	Collagen, type I, alpha 2	16.78
Thbs2	Thrombospondin 2	12.61
Col3a1	Collagen, type III, alpha 1	12.35
Ctgf	Connective tissue growth factor	12.24
Ccl12	Chemokine (C-C motif) ligand 12	10.31
Il1b	Interleukin 1 beta	10.27
Pdgfb	Platelet derived growth factor, B polypeptide	9.82
Thbs1	Thrombospondin 1	9.42
Cxcr4	Chemokine (C-X-C motif) receptor 4	9.32
Mmp14	Matrix metallopeptidase 14 (membrane-inserted)	8.89
Tnfa	Tumor necrosis factor alpha	7.57
Ccr2	Chemokine (C-C motif) receptor 2	6.73
Tgif1	TGFB-induced factor homeobox 1	6.51
Mmp2	Matrix metallopeptidase 2	5.62
Tgfb1	Transforming growth factor, beta 1	5.10
Ltbp1	Latent transforming growth factor beta binding protein 1	4.62
Ccl3	Chemokine (C-C motif) ligand 3	4.51
Mmp3	Matrix metallopeptidase 3	3.92
Edn1	Endothelin 1	3.53
Tgfbr2	Transforming growth factor, beta receptor II	3.52
Cebpb	CCAAT/enhancer binding protein (C/EBP), beta	3.52
Itgb8	Integrin beta 8	3.23
Snai1	Snail homolog 1 (Drosophila)	3.10
Mmp9	Matrix metallopeptidase 9	3.08
Itgav	Integrin alpha V	2.90
Plat	Plasminogen activator, tissue	2.84
Smad7	MAD homolog 7 (Drosophila)	2.54
Timp3	Tissue inhibitor of metalloproteinase 3	2.49
Tgfb3	Transforming growth factor, beta 3	2.47
Hgf	Hepatocyte growth factor	2.45
Itgb5	Integrin beta 5	2.37
Vegfa	Vascular endothelial growth factor A	–4.14
Agt	Angiotensinogen (serpin peptidase inhibitor, clade A, member 8)	–18.51
Egf	Epidermal growth factor	–26.01

RT^2 Profiler PCR Array was used to examine the expression of 84 genes closely associated with fibrosis in the ligated and contralateral SMGs (day 7). Positive and negative values represent increased and decreased fold expression of the genes of interest in the ligated SMGs compared to the contralateral SMGs, respectively. Data for genes whose expression was changed at least 2 fold were summarized. Data presented are average values from two independent experiments.

of *Ror2* and *Wnt5a* during renal fibrosis induced by UUO (Li *et al.*, 2013).

Previous report has shown that duct ligation of the SMG induces expression of TGF-β receptor I and activation of TGF-β/Smad signaling in acinar cells, indicating that acinar cells would be primary targets of TGF-β1 and TGF-β3 in the ligated SMG, even though the source of TGF-β production has not been identified (Woods *et al.*, 2015). Thus, it can be envisaged that acinar cells express TGF-β-target genes, such as *Serpine1*, a most highly upregulated gene in the ligated SMGs (Table I). Serpine1, also known as plasminogen activator inhibitor-1, contributes to tissue fibrosis of various organs by regulating epithelial-to-mesenchymal and/or endothelial-to-mesenchymal transition, or migration of inflammatory cells, depending on the cell types (Ghosh and Vaughan, 2012). *Ctgf* is another TGF-β-target gene that was also upregulated highly in the ligated SMGs (Table I). CTGF is a central mediator of tissue fibrosis in various organs, acting to generate myofibroblasts by modulating differentiation of epithelial cells, stellate cells, resident fibroblasts, or fibrocytes (Lipson *et al.*, 2012). It also activates the myofibroblasts to stimulate ECM deposition and tissue remodeling (Lipson *et al.*, 2012). Future studies will be necessary to clarify the roles of these and other upregulated genes in fibrosis of the SMGs.

Inflammation plays a fundamental role in tissue fibrosis (Wynn, 2007). In fact, previously reported evidence demonstrates that inflammatory cytokines, including TNF-α and IL-1β, play an essential role in the fibrosis of various tissues (Kamari *et al.*, 2011; Zhang *et al.*, 1997). Our PCR array and qRT-PCR analyses have revealed that expression of *TNF-α* and *IL-1β* is highly induced in the ligated SMGs. Importantly, we have recently shown that TNF-α and IL-1β induce expression of *Ror1* and *Ror2* in injured skeletal muscles in mice (Kamizaki *et al.*, 2017). Furthermore, IL1-β has been shown to induce expression of *Wnt5a* and *Ror2* in human mesenchymal stem cells (Sonomoto *et al.*, 2012), suggesting that these inflammatory cytokines might be involved in expression of *Ror1*, *Ror2*, and *Wnt5a* in the ligated SMGs undergoing fibrosis. It is currently unknown which cells within the ligated SMGs are major source of these inflammatory cytokines.

The ductal ligation induces expression of *MMP-2*, a ubiquitous metalloproteinase that is involved in various biological processes, such as inflammation, wound healing, and tumor invasion (Lovett *et al.*, 2013; Yang *et al.*, 2017; Zhang *et al.*, 2016). We have previously shown that Ror2 is required for induced expression of MMP-2 during renal fibrosis induced by UUO (Li *et al.*, 2013), suggesting that Ror2-mediated signaling might induce expression of *MMP-2* in the ligated SMGs to regulate fibrosis. Despite the fact that Ror1 plays essential roles in tissue- and organogenesis during embryonic development and cancer progression (Endo *et al.*, 2015; Minami *et al.*, 2010), its roles in tissue-damage responses have not been reported, except for our recent finding about the critical role of Ror1 during regeneration of the injured skeletal muscles (Kamizaki *et al.*, 2017). Since the SMGs have capacity to regenerate after long-term obstruction (Watanabe *et al.*, 2017), it would be of interest to examine a possible functional implication of Ror1 in regeneration of the damaged SMGs.

In summary, we found that the ductal ligation induces expression of *Ror1*, *Ror2*, and *Wnt5a* in the SMGs undergoing fibrosis, which is accompanied by robust expression of fibrosis-associated genes, such as *TGF-β1*, *TNF-α*, *IL-1β*, and *MMP-2*. Increased immunostaining signals of Ror2 were detected in the fibrotic lesions with abundant accumulation of fibroblastic cells, fibroblasts and collagen fibers in the ligated SMGs, suggesting that Ror2-mediated signaling might be activated in response to tissue damage and involved in the progression of fibrosis within the SMGs. Further studies will be required to understand the

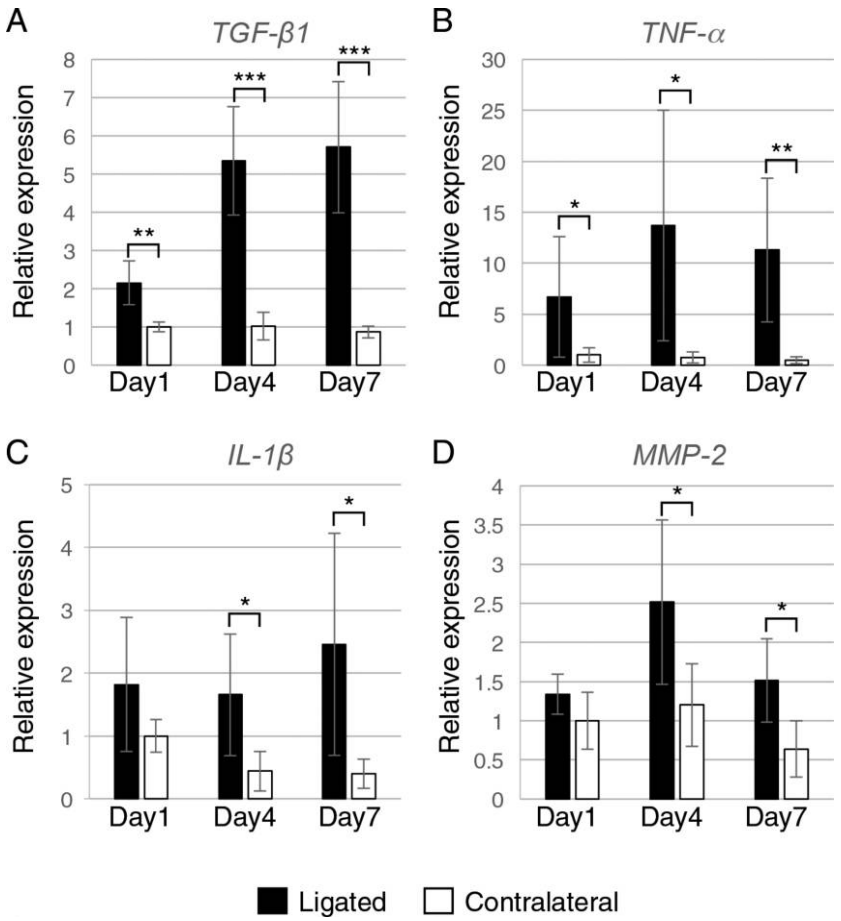

Fig. 5. Effects of the ductal ligation on expression levels of *TGF-β1*, *TNF-α*, *IL-1β*, and *MMP-2*. The ligated and contralateral SMGs were isolated on day 1, 4, and 7 after the ductal ligation and analyzed by qRT-PCR. Data represent means±SD (n=6). *P<0.05; **P<0.005; ***P<0.0005, *t* test.

exact functional roles of Ror1, Ror2, and Wnt5a during fibrosis of the SMGs.

Acknowledgments. We are grateful to Akira Tanaka and Kazuyoshi Murayama (The Nippon Dental University at Niigata) for their critical information about the main excretory duct ligation technique. This work was supported by grants-in-aid for Scientific Research (B) [16H05152 (Y.M.)] from MEXT.

References

Endo, M., Nishita, M., Fujii, M., and Minami, Y. 2015. Insight into the role of Wnt5a-induced signaling in normal and cancer cells. *Int. Rev. Cell Mol. Biol.*, **314**: 117–148.

Endo, M., Ubulkasim, G., Kobayashi, C., Onishi, R., Aiba, A., and Minami, Y. 2017. Critical role of Ror2 receptor tyrosine kinase in regulating cell cycle progression of reactive astrocytes following brain injury. *Glia*, **65**: 182–197.

Fox, R.I., Stern, M., and Michelson, P. 2000. Update in Sjogren syndrome. *Curr. Opin. Rheumatol.*, **12**: 391–398.

Ghosh, A.K. and Vaughan, D.E. 2012. PAI-1 in tissue fibrosis. *J. Cell. Physiol.*, **227**: 493–507.

He, X., Semenov, M., Tamai, K., and Zeng, X. 2004. LDL receptor-related proteins 5 and 6 in Wnt/beta-catenin signaling: arrows point the way. *Development*, **131**: 1663–1677.

Henson, B.S., Inglehart, M.R., Eisbruch, A., and Ship, J.A. 2001. Preserved salivary output and xerostomia-related quality of life in head and neck cancer patients receiving parotid-sparing radiotherapy. *Oral Oncol.*, **37**: 84–93.

Hurlstone, A. and Clevers, H. 2002. T-cell factors: turn-ons and turn-offs. *Embo J.*, **21**: 2303–2311.

Kamari, Y., Shaish, A., Vax, E., Shemesh, S., Kandel-Kfir, M., Arbel, Y., Olteanu, S., Barshack, I., Dotan, S., Voronov, E., Dinarello, C.A., Apte, R.N., and Harats, D. 2011. Lack of interleukin-1alpha or interleukin-1beta inhibits transformation of steatosis to steatohepatitis and liver fibrosis in hypercholesterolemic mice. *J. Hepatol.*, **55**: 1086–1094.

Kamizaki, K., Doi, R., Hayashi, M., Saji, T., Kanagawa, M., Toda, T., Fukada, S.I., Ho, H.H., Greenberg, M.E., Endo, M., and Minami, Y. 2017. The Ror1 receptor tyrosine kinase plays a critical role in regulating satellite cell proliferation during regeneration of injured muscle. *J. Biol. Chem.*, **292**: 15939–15951.

Kani, S., Oishi, I., Yamamoto, H., Yoda, A., Suzuki, H., Nomachi, A., Iozumi, K., Nishita, M., Kikuchi, A., Takumi, T., and Minami, Y. 2004. The receptor tyrosine kinase Ror2 associates with and is activated by casein kinase Iepsilon. *J. Biol. Chem.*, **279**: 50102–50109.

Kikuchi, A. and Yamamoto, H. 2008. Tumor formation due to abnormalities in the beta-catenin-independent pathway of Wnt signaling. *Cancer*

Sci., **99**: 202–208.

Kohn, A.D. and Moon, R.T. 2005. Wnt and calcium signaling: beta-catenin-independent pathways. *Cell Calcium*, **38**: 439–446.

Li, X., Yamagata, K., Nishita, M., Endo, M., Arfian, N., Rikitake, Y., Emoto, N., Hirata, K., Tanaka, Y., and Minami, Y. 2013. Activation of Wnt5a-Ror2 signaling associated with epithelial-to-mesenchymal transition of tubular epithelial cells during renal fibrosis. *Genes Cells*, **18**: 608–619.

Lipson, K.E., Wong, C., Teng, Y., and Spong, S. 2012. CTGF is a central mediator of tissue remodeling and fibrosis and its inhibition can reverse the process of fibrosis. *Fibrogenesis Tissue Repair*, **5**: S24.

Liu, Y. 2006. Renal fibrosis: new insights into the pathogenesis and therapeutics. *Kidney Int.*, **69**: 213–217.

Lovett, D.H., Mahimkar, R., Raffai, R.L., Cape, L., Zhu, B.Q., Jin, Z.Q., Baker, A.J., and Karliner, J.S. 2013. N-terminal truncated intracellular matrix metalloproteinase-2 induces cardiomyocyte hypertrophy, inflammation and systolic heart failure. *PLoS One*, **8**: e68154.

Mallat, A. and Lotersztajn, S. 2013. Cellular mechanisms of tissue fibrosis. 5. Novel insights into liver fibrosis. *Am. J. Physiol. Cell Physiol.*, **305**: C789–799.

Minami, Y., Oishi, I., Endo, M., and Nishita, M. 2010. Ror-family receptor tyrosine kinases in noncanonical Wnt signaling: Their implications in developmental morphogenesis and human diseases. *Dev. Dyn.*, **239**: 1–15.

Murakami, M., Nishi, Y., Seto, K., Kamashita, Y., and Nagaoka, E. 2015. Dry mouth and denture plaque microflora in complete denture and palatal obturator prosthesis wearers. *Gerodontology*, **32**: 188–194.

Nishita, M., Enomoto, M., Yamagata, K., and Minami, Y. 2010. Cell/tissue-tropic functions of Wnt5a signaling in normal and cancer cells. *Trends Cell Biol.*, **20**: 346–354.

Pedersen, A.M., Bardow, A., Jensen, S.B., and Nauntofte, B. 2002. Saliva and gastrointestinal functions of taste, mastication, swallowing and digestion. *Oral Dis.*, **8**: 117–129.

Sato, A., Kayama, H., Shojima, K., Matsumoto, S., Koyama, H., Minami, Y., Nojima, S., Morii, E., Honda, H., Takeda, K., and Kikuchi, A. 2015. The Wnt5a-Ror2 axis promotes the signaling circuit between interleukin-12 and interferon-gamma in colitis. *Sci. Rep.*, **5**: 10536.

Shimizu, T., Smits, R., and Ikenaka, K. 2016. Microglia-induced activation of non-canonical Wnt signaling aggravates neurodegeneration in demyelinating disorders. *Mol. Cell. Biol.*, **36**: 2728–2741.

Shimizu, Y., Yamamoto, M., Naishiro, Y., Sudoh, G., Ishigami, K., Yajima, H., Tabeya, T., Matsui, M., Suzuki, C., Takahashi, H., Seki, N., Himi, T., Yamashita, K., Noguchi, H., Hasegawa, T., Suzuki, Y., Honda, S., Abe, T., Imai, K., and Shinomura, Y. 2013. Necessity of early intervention for IgG4-related disease--delayed treatment induces fibrosis progression. *Rheumatology (Oxford)*, **52**: 679–683.

Sonomoto, K., Yamaoka, K., Oshita, K., Fukuyo, S., Zhang, X., Nakano, K., Okada, Y., and Tanaka, Y. 2012. Interleukin-1beta induces differentiation of human mesenchymal stem cells into osteoblasts via the Wnt-5a/receptor tyrosine kinase-like orphan receptor 2 pathway. *Arthritis Rheum.*, **64**: 3355–3363.

Tatler, A.L. and Jenkins, G. 2012. TGF-beta activation and lung fibrosis. *Proc. Am. Thorac. Soc.*, **9**: 130–136.

Thenappan, A., Li, Y., Kitisin, K., Rashid, A., Shetty, K., Johnson, L., and Mishra, L. 2010. Role of transforming growth factor beta signaling and expansion of progenitor cells in regenerating liver. *Hepatology*, **51**: 1373–1382.

Veeman, M.T., Axelrod, J.D., and Moon, R.T. 2003. A second canon. Functions and mechanisms of beta-catenin-independent Wnt signaling. *Dev. Cell*, **5**: 367–377.

Vissink, A., Mitchell, J.B., Baum, B.J., Limesand, K.H., Jensen, S.B., Fox, P.C., Elting, L.S., Langendijk, J.A., Coppes, R.P., and Reyland, M.E. 2010. Clinical management of salivary gland hypofunction and xerostomia in head-and-neck cancer patients: successes and barriers. *Int. J. Radiat. Oncol. Biol. Phys.*, **78**: 983–991.

Watanabe, H., Takahashi, H., Hata-Kawakami, M., and Tanaka, A. 2017. Expression of c-kit and Cytokeratin 5 in the Submandibular Gland after Release of Long-Term Ligation of the Main Excretory Duct in Mice. *Acta Histochem. Cytochem.*, **50**: 111–118.

Wodarz, A. and Nusse, R. 1998. Mechanisms of Wnt signaling in development. *Annu. Rev. Cell Dev. Biol.*, **14**: 59–88.

Woods, L.T., Camden, J.M., El-Sayed, F.G., Khalafalla, M.G., Petris, M.J., Erb, L., and Weisman, G.A. 2015. Increased Expression of TGF-beta Signaling Components in a Mouse Model of Fibrosis Induced by Submandibular Gland Duct Ligation. *PLoS One*, **10**: e0123641.

Wynn, T.A. 2007. Common and unique mechanisms regulate fibrosis in various fibroproliferative diseases. *J. Clin. Invest.*, **117**: 524–529.

Yang, L., Zheng, Z., Zhou, Q., Bai, X., Fan, L., Yang, C., Su, L., and Hu, D. 2017. miR-155 promotes cutaneous wound healing through enhanced keratinocytes migration by MMP-2. *J. Mol. Histol.*, **48**: 147–155.

Zhang, K., Gharaee-Kermani, M., McGarry, B., Remick, D., and Phan, S.H. 1997. TNF-alpha-mediated lung cytokine networking and eosinophil recruitment in pulmonary fibrosis. *J. Immunol.*, **158**: 954–959.

Zhang, S., Ma, J., Fu, Z., Zhang, Z., Cao, J., Huang, L., Li, W., Xu, P., and Cao, X. 2016. Promotion of breast cancer cells MDA-MB-231 invasion by di(2-ethylhexyl)phthalate through matrix metalloproteinase-2/-9 overexpression. *Environ. Sci. Pollut. Res. Int.*, **23**: 9742–9749.

(Received for publication, September 13, 2017, accepted, October 19, 2017 and published online, October 25, 2017)